# Magnetic Resonance Spectroscopy of Triplet-State Organic Molecules in Zero External Magnetic Field

Cite as: J. Chem. Phys. **53**, 1906 (1970); https://doi.org/10.1063/1.1674268
Submitted: 01 April 1970 . Published Online: 18 September 2003

Clyde A. Hutchison, John V. Nicholas, and Gary W. Scott

# Magnetic Resonance Spectroscopy of Triplet-State Organic Molecules in Zero External Magnetic Field*,†

CLYDE A. HUTCHISON JR., JOHN V. NICHOLAS,‡ AND GARY W. SCOTT§
*Enrico Fermi Institute and Department of Chemistry, University of Chicago, Chicago, Illinois 60637*

(Received 1 April 1970)

Some derivations are given for approximations to the energy levels and eigenstates of triplet-state organic molecules in external magnetic fields of such a magnitude that the electron Zeeman interaction is small relative to the intramolecular electron–electron interaction. An exact calculation of the exactly zero external field magnetic resonance spectrum of photoexcited naphthalene is given. Experimental measurements of the zero-field spectrum of naphthalene are presented. The results of the approximate and exact treatments are compared with these results and with other available experimental information.

## I. INTRODUCTION

For several years many workers[1–22] have recognized important features of the magnetic dipole spectra of triplet-state organic molecules in weak external magnetic fields of such a magnitude that the electron Zeeman interaction is small relative to the intramolecular electron–electron interaction. Such spectra are easily observable with relatively large signal intensities, in the case of a photoexcited aromatic molecule, for example, because of the relatively large electron energy splittings in the absence of an external magnetic field, and have been studied by several investigators[1–22] by means of electron paramagnetic resonance spectroscopy (EPR).

In this paper we summarize some derivations of approximations to the energy levels and transition probabilities to be expected at these low fields on the basis of the well-known facts concerning the triplet states of organic molecules. We make a number of comparisons of these expectations with experimental observations on EPR line structures, shapes, and intensities. We also present the results of an exact calculation of the exactly zero external magnetic field spectrum of photoexcited naphthalene and compare this calculation with the experimental results. The matters discussed here have important applications in both electron nuclear double resonance (ENDOR) and EPR studies at very small fields.

## II. APPROXIMATE TREATMENTS

### A. The Spin Hamiltonian

The magnetic resonance spectra of aromatic hydrocarbon molecules in triplet states may be described in terms of the eigenvalues and eigenstates of the spin Hamiltonian operator,[9]

$$\mathcal{H}=\mathcal{H}_1+\mathcal{H}_2+\mathcal{H}_3+\mathcal{H}_4$$
$$=+\mathbf{G}\cdot\mathbf{S}+\mathbf{S}\cdot\mathsf{T}\cdot\mathbf{S}+\sum_k \mathbf{\mathcal{G}}\cdot\mathbf{I}_k+\sum_k \mathbf{S}\cdot\mathsf{A}_k\cdot\mathbf{I}_k, \quad (1)$$

in which $S=1$, $\mathbf{I}_k$ is the dimensionless nuclear spin of the $k$th proton in the molecule, $I_k=\frac{1}{2}$, all $k$, $\mathbf{G}\equiv+|\beta_e|\mathbf{H}_0\cdot\mathbf{g}_e$, $\mathsf{T}$ is the fine structure tensor, $\mathbf{\mathcal{G}}\equiv-|\beta_n|\mathbf{H}_0\cdot\mathbf{g}_n$, $\mathsf{A}_k$ is the hyperfine interaction tensor for the $k$th proton, and $\mathbf{g}_e$ and $\mathbf{g}_n$ are the Zeeman tensors for the electrons and the nuclei, respectively.

In some parts of what follows we will assume that the principal axes of $\mathbf{g}_e$ are coincident with those of $\mathsf{T}$. Inasmuch as both of these sets of axes must be coincident with molecular symmetry axes such as those shown in Fig. 1, and inasmuch as the actual deviations of molecules in crystals from such idealized symmetry are very small indeed, this assumption will introduce only negligible errors into our present considerations.

The form $\mathbf{G}\cdot\mathbf{S}$ is general for $\mathcal{H}_1$, but if $\mathbf{g}_e$ is not isotropic, then the $\mathsf{A}_k$ are not, in general, symmetric tensors. In some discussions given below we assume the $\mathsf{A}_k$ to be symmetric. The errors introduced by this assumption are considered in Sec. IV.B below.

We will assume that $\mathbf{g}_n$ is an isotropic tensor.

Inasmuch as the electronic states which we will be considering lie far from other paramagnetic electronic states, this is an extremely good assumption for our purposes.

We will not consider direct interactions between the protons. These interactions are much smaller than the expectation value, $\langle\mathcal{H}_4\rangle$. $\mathcal{H}_4$ itself provides, of course, an indirect mechanism for the interactions of the protons with each other through their interactions with the electrons.

In considering the application of the spin Hamiltonian, Eq. (1), to magnetic resonance experiments, we may give our attention to three ranges of values of external magnetic field strengths which are customarily used in such studies. For each of these three ranges we find convenient approximate methods for using Eq. (1). We make the division according to the sizes of $|\mathbf{G}|$ and $|\mathbf{\mathcal{G}}|$ with respect to the sizes of $|T_{ii}|$ and $|A_{kjj}|$, $i,j=x,y,z$, in (1) for a typical molecule, such as naphthalene in its lowest triplet state. For this molecule[9,23,24] $|T_{zz}+T_{xx}|/h\cong3.0\times10^9$ Hz$\cong|T_{zz}|/h$ and $|A_{kxx}|/h\cong1.5\times10^7$ Hz for an $\alpha$ proton, i.e., $k=1$, 4, 5, or 8.

Thus we have $|T_{zz}|/|A_{kxx}|\cong200$. It should also be noted that $|\mathbf{G}|/|\mathbf{\mathcal{G}}|\cong650$ (for all values of $|\mathbf{G}|$). The three ranges are selected as follows:

High-field range: We define this range by

$$|\mathbf{G}|>|T_{zz}|. \quad (2)$$

This requires that $|\mathbf{H}_0|$ be greater than 1000 G.[9] At this lower limit we then have $|\mathcal{G}|/h \cong 5\times10^6$ Hz, which may be compared with $|A_{kxx}|/h \cong 1.5\times10^7$ Hz for naphthalene $\alpha$ protons.

Low-field range: We define this range by

$$|\mathbf{G}| > |A_{kxx}|,$$
$$|\mathcal{G}| < (1/10)\,|A_{kxx}|. \tag{3}$$

This requires that 350 G$> |\mathbf{H}_0| >$5 G in the case of naphthalene $\alpha$ protons.[9,24] It also requires that $1.5\times10^6$ Hz$> |\mathcal{G}|/h > \times10^4$ Hz.

Almost-zero-field range: We define this range by

$$|A_{kxx}| > |\mathbf{G}|. \tag{4}$$

This requires that $|\mathbf{H}_0| <$5 G[9,24] and that $|\mathcal{G}|/h < 2\times10^4$ Hz.

### B. The High-Field Range [See Eq. (2)]

The approximation which is useful in this range has been discussed in considerable detail.[9,25] It has been used[25–27] in the treatment of the conventional high-field experimental ENDOR results and EPR results for organic molecules in triplet states in single crystals and is reviewed here.

The three states which diagonalize $\mathcal{H}_1+\mathcal{H}_2$ [in (1)] in a conventional EPR or ENDOR experiment when $|\mathbf{H}_0|$ is larger than 1000 G are labeled by $N_1$, $N_2$, and $N_3$. A matrix element of $\mathcal{H}_4$ which is diagonal in $N$ may be written as

$$\langle N_i|\,\mathcal{H}_1\,|N_i\rangle = \langle\mathbf{S}\rangle_{N_i}\cdot\sum\mathbf{A}_k\cdot\mathbf{I}_k, \tag{5}$$

in which $\langle\mathbf{S}\rangle_{N_i}$ denotes the expectation value of $\mathbf{S}$ in electron state $N_i$. $\langle\mathbf{S}\rangle_{N_i}$ may be simply calculated from the measured principal values of $\mathbf{g}_e$ and $\mathbf{T}$ and the measured $\mathbf{G}$.

The approximation which is useful in this case consists of the neglecting of the matrix elements, $\langle N_i|\,\mathcal{H}_4\,|N_j\rangle$, $i\neq j$. We may then choose the axis of nuclear (proton) spin quantization to lie in the direction of

$$^{\text{eff}}\mathcal{G}_k \equiv \mathcal{G} + \langle\mathbf{S}\rangle_N\cdot\mathbf{A}_k, \tag{6}$$

i.e., in the direction of the magnetic field seen by the $k$th proton in this approximation, and we may take the individual nuclear states to be the $+\frac{1}{2}$ and $-\frac{1}{2}$ spin states in this field, $^{\text{eff}}\mathcal{G}_k$, i.e., the eignestates of $^{\text{eff}}\mathcal{G}_k\cdot\mathbf{I}_k$.

Thus, the $k$th proton's ENDOR shift, $\Delta\nu_k$ (i.e., the $k$th proton's ENDOR frequency minus the proton gaussmeter frequency in the same field), is given by

$$h\Delta\nu_k = |\,^{\text{eff}}\mathcal{G}_k| - g_n|\beta_n|\,|\mathbf{H}_0|, \tag{7}$$

and the $k$th proton's frequency splitting, $|\Delta\nu_k|$, of an EPR line for the electronic transition $|N_i\rangle\rightarrow|0\rangle$ by

$$h|\Delta\nu_k| = \big|\,|\,^{\text{eff}}\mathcal{G}_k| - g_n|\beta_n|\,|\mathbf{H}_0|\,\big|. \tag{8}$$

The quantities described by the right sides of (7) and (8) are the ones directly observed in high-field ENDOR and EPR spectra, respectively.

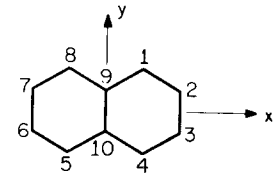

FIG. 1. Naphthalene molecule.

It is well known that $\langle\mathbf{S}\rangle_N\rightarrow0$ as $|\mathbf{H}_0|\rightarrow0$. Thus in this high-field approximation $^{\text{eff}}\mathcal{G}\rightarrow0$ as $|\mathbf{H}_0|\rightarrow0$ and so, also, does $h\Delta\nu_k$. Hence in this approximation [see (6) above] ENDOR shifts, and hyperfine structures of EPR spectra, vanish at zero external field. It is, of course, to be noted here that the invariance of $\mathcal{H}_2+\mathcal{H}_4$ under time reversal requires that both expectation values, $\langle\mathbf{S}\rangle$ and $\langle\mathbf{I}_k\rangle$, be zero, but the expectation value $\langle\mathbf{S}\cdot\mathbf{A}_k\cdot\mathbf{I}_k\rangle$ is not required to vanish, and thus hyperfine interactions may be greater than zero at zero external magnetic field.

### C. The Low-Field Range [See Eq. (3)]

Inasmuch as in this range $|\mathcal{G}|$ is always much smaller than $|\mathbf{G}|$, $|T_{zz}|$, or $|A_{kxx}|$, we wish first to diagonalize $\mathcal{H}_1+\mathcal{H}_2+\mathcal{H}_4$ and to treat $\mathcal{H}_3$ as a perturbation. For an arbitrary molecule it is certainly not possible to effect this diagonalization easily. Nevertheless, in particular situations, including some of those which have been studied experimentally,[16] it is possible to obtain, in a simple manner, approximate diagonalizations which describe the experimental situation with great accuracy.

Our first particularization is to the case in which all of the tensors in $\mathcal{H}_4$ may be written as

$$\mathbf{A}_k = \begin{pmatrix} A_{kxx} & A_{kxy} & 0 \\ A_{kxy} & A_{kyy} & 0 \\ 0 & 0 & A_{kzz} \end{pmatrix}, \tag{9}$$

in which $x$, $y$, and $z$ refer to the principal axes of the tensor $\mathbf{T}$ in $\mathcal{H}_2$. Such is the case, for example, for photo-excited naphthalene, benzene, etc.,[24–26] in the approximation in which they are considered to be planar molecules, and the $z$ axis lies normal to the plane. We may then express the terms in (1) as

$$\mathcal{H}_1 = G_xS_x+G_yS_y+G_zS_z,$$
$$\mathcal{H}_2 = DS_z^2+E(S_x^2-S_y^2),$$
$$\mathcal{H}_3 = \sum_k\{\mathcal{G}_xI_{kx}+\mathcal{G}_yI_{ky}+\mathcal{G}_zI_{kz}\},$$
$$\mathcal{H}_4 = {}^x\mathcal{H}_4+{}^y\mathcal{H}_4+{}^z\mathcal{H}_4,$$
$${}^x\mathcal{H}_4 \equiv \sum_k\{S_x[A_{kxx}I_{kx}+A_{kxy}I_{ky}]\},$$
$${}^y\mathcal{H}_4 \equiv \sum_k\{S_y[A_{kyy}I_{ky}+A_{kxy}I_{kx}]\},$$
$${}^z\mathcal{H}_4 \equiv \sum_k S_zA_{kzz}I_{kz}. \tag{10}$$

Our second particularization is to the case when $\mathbf{H}_0$ is parallel to a principal axis of the tensor $\mathsf{T}$ in $\mathcal{H}_2$. We take $\hat{\mathbf{x}}$, $\hat{\mathbf{y}}$, and $\hat{\mathbf{z}}$ to be unit vectors along the principal axes of $\mathsf{T}$. It is, for example, a simple matter to diagonalize $\mathcal{H}_1+\mathcal{H}_2+{}^x\mathcal{H}_4$ for the case in which $\mathbf{H}_0\cdot\hat{\mathbf{x}}=|\mathbf{H}_0|$, and this statement also holds when $y$ or $z$ are substituted for $x$. For the example $\mathbf{H}_0\cdot\hat{\mathbf{x}}=|\mathbf{H}_0|$, $D-E$ is an eigenvalue of $\mathcal{H}_1+\mathcal{H}_2$ only, for all values of $|\mathbf{H}_0|$. The other two eigenvalues, of $\mathcal{H}_1+\mathcal{H}_2$ only, are $\frac{1}{2}\{D+E\pm[(D+E)^2+4G_x^2]^{1/2}\}$. If there are $n$ protons, each of these three eigenvalues is $2^n$-fold degenerate. When we consider $\mathcal{H}_1+\mathcal{H}_2+{}^x\mathcal{H}_4$ we may choose nuclear spin states for the $k$th proton which diagonalize the operator, $A_{kxx}I_x+A_{kxy}I_y$. It is then easily seen that the eigenvalues of $\mathcal{H}_1+\mathcal{H}_2+{}^x\mathcal{H}_4$ are

$$2^n \text{ eigenvalues each equal to } D-E, \tag{11}$$

and

$$2\times 2^n \text{ eigenvalues given by } \tfrac{1}{2}\Big(D+E\pm\{(D+E)^2+4[G_x+\tfrac{1}{2}\sum_k(\pm)\,|\,A_{kxx}+iA_{kxy}\,|]^2\}^{1/2}\Big), \tag{12}$$

in which $\sum_k(\pm)$ denotes a sum with a particular choice of $+$ or $-$ sign for each of the $n$ terms. There are $2^n$ such particular choices and hence $2^n\times 2$ eigenvalues.

In a similar manner we see that in the case in which $\mathbf{H}_0\cdot\hat{\mathbf{z}}=|\mathbf{H}_0|$, the eigenvalues of $\mathcal{H}_1+\mathcal{H}_2+{}^z\mathcal{H}_4$ are

$$2^n \text{ eigenvalues equal to zero,} \tag{13}$$

and

$$2\times 2^n \text{ eigenvalues given by } D\pm\{E^2+[G_z+\tfrac{1}{2}\sum_k(\pm)A_{kzz}]^2\}^{1/2}. \tag{14}$$

In the case of (11) and (12) for $\mathbf{H}_0\cdot\hat{\mathbf{x}}=|\mathbf{H}_0|$, the omission of ${}^y\mathcal{H}_4$ and ${}^z\mathcal{H}_4$ introduces only small errors, which amount, for example, in the case of photoexcited naphthalene[9] to 2–25 kHz, over the low-field range defined by (3). $\mathcal{H}_3$ makes a contribution, in this example, of 20–1500 kHz over the low-field range, but for purposes of discussing EPR spectra it may be neglected inasmuch as its effect on the two levels involved in the EPR transition cancel each other. Similar statements concerning the size and effects of the neglected terms hold for the other principal axis directions of $\mathbf{H}_0$.

When we consider an EPR spectrum obtained by scanning the magnetic field $|\mathbf{H}_0|$, keeping the frequency $\nu$ constant, we see that (11) and (12), or (13) and (14), give very simple expressions for the contributions of each proton to the hyperfine pattern. We describe these contributions in terms of the conventional "field splitting" by the $k$th proton. With $\mathbf{H}_0$ parallel to $\hat{\mathbf{x}}$, $\hat{\mathbf{y}}$, or $\hat{\mathbf{z}}$, we obtain, for these splittings the values

$$\Delta G_{kx}=|\,A_{kxx}+iA_{kxy}\,|,$$
$$\Delta G_{ky}=|\,A_{kyy}+iA_{kxy}\,|,$$
$$\Delta G_{kz}=|\,A_{kzz}\,|, \tag{15}$$

respectively.

In this low-field region we are in a range of field strengths in which the plots of energy $W$ vs field strength $|\mathbf{H}_0|$ are strongly curved, i.e., $\langle\mathbf{S}\rangle$ is changing rapidly as $|\mathbf{H}_0|$ changes (see Fig. 4, p. 70, Ref. 9). The transformation from the case of frequency scan with constant field to the case of field scan with constant frequency is not so simple as in the high-field case where the energy is linear in the field, i.e., where $\langle\mathbf{S}\rangle$ is constant. However, the expressions (15) show that within our approximation the field splitting of the $k$th proton is independent of the field strength $|\mathbf{H}_0|$. For the case $\mathbf{H}_0$ parallel to $\hat{\mathbf{z}}$ and (9) valid, the third equation of (15) is exact. For the other two cases the relations (15) are correct within 1% for the lowest triplet state of naphthalene. For triplet-state molecules as $|\mathbf{H}_0|$ is decreased through the low-field range, the increasing value of $d|\mathbf{H}_0|/dW$, the change in field required for a given change in energy, is just compensated by the decreasing value of the energy splitting by the $k$th proton. In other words, as the expectation value $\langle\mathbf{S}\rangle$ of the spin changes through the low-field region the hyperfine energy splitting varies as $\langle\mathbf{S}\rangle$ and the change of $|\mathbf{H}_0|$ required to obtain a given change of energy varies as $\langle\mathbf{S}\rangle^{-1}$.

The consequence of these effects is that the EPR hyperfine patterns in the low-field range will be very similar to those in the high-field case.

### D. The Almost-Zero-Field Range

At exactly zero external field we may consider $\mathcal{H}_4$ to be a perturbation added to $\mathcal{H}_2$ and treat the problem by second-order perturbation theory, noting that $\mathcal{H}_4$ has no matrix elements between any two of the $2^n$ degenerate eigenstates associated with an eigenvalue of $\mathcal{H}_2$. We denote the electronic eigenstates of $\mathcal{H}_2$ by

$$|+\rangle\equiv(|+1\rangle+|-1\rangle)/\sqrt{2},$$
$$|-\rangle\equiv(|+1\rangle-|-1\rangle)/\sqrt{2},$$
$$|0\rangle\equiv|0\rangle, \tag{16}$$

in which

$$S_z|+1\rangle=|+1\rangle,\ S_z|-1\rangle=-|-1\rangle,\ S_z|0\rangle=0.$$

Each of these states, (16) is to be multiplied by each of the $2^n$ proton spin states ($n$ is the number of protons) to give the molecule spin states. We generate a nuclear spin Hamiltonian for each of the three states, (16), in the usual manner. For example, the nuclear spin Hamiltonian $\mathcal{H}_{I+}$ for the $2^n$-dimensional manifold

associated with the electron state $|+\rangle$ is given by

$$\mathcal{H}_{I+}=\frac{|\langle+|S_x\Lambda_x+S_y\Lambda_y+S_z\Lambda_z|-\rangle|^2}{2E}+\frac{|\langle+|S_x\Lambda_x+S_y\Lambda_y+S_z\Lambda_z|0\rangle|^2}{D+E}$$
$$=\langle+|S_z^2|+\rangle(\Lambda_z^2/2E)+\langle+|S_x^2|+\rangle\times[\Lambda_x^2/(D+E)]$$
$$=(2E)^{-1}\Lambda_z^2+(D+E)^{-1}\Lambda_x^2, \quad (17)$$

in which

$$\Lambda_x\equiv\sum_k(A_{kxx}I_{kx}+A_{kxy}I_{ky}),$$
$$\Lambda_y\equiv\sum_k(A_{kyy}I_{ky}+A_{kxy}I_{ky}),$$
$$\Lambda_z\equiv\sum_k A_{kzz}I_{kz}.$$

The eigenvalues and eigenstates of the three nuclear spin Hamiltonians when each is diagonalized within the $2^n$-dimensional manifold of nuclear states gives us our approximations to the solutions at exactly zero external magnetic field. The use of the nuclear spin Hamiltonian of course greatly reduces the size of this secular problem relative to that of the exact problem. The errors in energy levels introduced by this approximation are 1 kHz or less in the case of a molecule such as naphthalene[9,24] in its lowest triplet state.

If we now consider the application of a magnetic field in the almost-zero-field range defined by (4), we may use second-order perturbation theory to treat $\mathcal{H}_1+\mathcal{H}_3$. We then obtain for our nuclear spin Hamiltonian for the $2^n$-dimensional manifold associated with the electron state $|+\rangle$ the following expression when, for example, $\mathbf{H}_0$ is parallel to $\hat{\mathbf{z}}$:

$$\mathcal{H}_{I+}=(1/2E)(G_z^2+2G_z\Lambda_z+\Lambda_z^2)+\sum_k\mathcal{G}_{kz}I_z+(D+E)^{-1}\Lambda_x^2. \quad (18)$$

The eigenvalues and eigenstates in the $2^n$-dimensional manifolds of this and the other two similar spin Hamiltonians give us our approximations to the solutions for the almost-zero-field region when $\mathbf{H}_0$ is parallel to $\hat{\mathbf{z}}$. In a similar manner we obtain expressions for the cases when $\mathbf{H}_0$ is parallel to $\hat{\mathbf{x}}$ or $\hat{\mathbf{y}}$.

We may consider the application of this approximation at exactly zero field for simple cases. In the simplest case of a triplet-state molecule with hyperfine interaction produced by only a single proton, there is no degeneracy removal. Each electron state remains twofold degenerate and thus this case is not of immediate experimental interest, there being no hyperfine structure of the absorption lines.

Therefore, as a simplest significant illustrative example we may consider the case of a triplet-state molecule with only two protons. We assume that both of these protons have tensors $\mathbf{A}_k$ of the form (9). In this case the approximation gives for the shifts $\Delta W$ of energy from the eigenvalues of $\mathcal{H}_2$, produced by $\mathcal{H}_4$, the following expressions:

electron state $|+\rangle$:

$$\Delta W_+=[1/4(D+E)](|A_{1xx}+iA_{1xy}|\pm|A_{2xx}+iA_{2xy}|)^2+(1/8E)(A_{1zz}\pm A_{2zz})^2; \quad (19)$$

electron state $|0\rangle$:

$$\Delta W_0=-[1/4(D+E)](|A_{1xx}+iA_{1xy}|\pm|A_{2xx}+iA_{2xy}|)^2-[1/4(D-E)](|A_{1yy}+iA_{1xy}|\pm|A_{2yy}+iA_{2xy}|)^2; \quad (20)$$

electron state $|-\rangle$:

$$\Delta W_-=+[1/4(D-E)]\times(|A_{1yy}+iA_{1xy}|\pm|A_{2yy}+iA_{2xy}|)^2-(1/8E)(A_{1zz}\pm A_{2zz})^2. \quad (21)$$

In the above expressions, all possible sets of + and − signs are to be used to give the four values for each of the four-dimensional nuclear manifolds.

Two important features of the EPR absorption spectra at exactly zero field are apparent from this example.

(I) We see from (21) that the shifts of all of the levels associated with the electron state $|-\rangle$ are positive for a molecule such as naphthalene in its lowest triplet state in which $|D|>|E|$ and $D$ is + and $E$ is −. Equation (20) shows that the shifts for the state $|0\rangle$ are all negative. It is thus clear that the centers of gravity of the absorption lines at zero external field are shifted by the hyperfine interaction. Thus values of $D$ and $E$ determined directly from absorption maxima at zero field, not taking these shifts into account, are in error, e.g., the frequency $\nu_{\max}(-,0)$ of maximum absorption for the transition $|-\rangle\leftrightarrow|0\rangle$ does not satisfy $D-E=h\nu_{\max}(-,0)$. These shifts, in the case of naphthalene,[9,24] correspond to approximately 0.2 MHz in peak position, an easily measurable magnitude. On the other hand, this error has a magnitude about equal to that of the change in absorption frequency per 1°K.[28]

(II) It is clear from an expression such as (21) that the largest proton hyperfine frequency splitting is approximately equal to $(\sum_k A_{kzz})^2/4Eh$, this being twice the largest term in (21). For naphthalene[9,24] in its lowest triplet state $(\sum_k A_{kzz})^2/h^2$ is approximately $(65\text{ MHz})^2$, and when this value is divided by $4E/h$ the result is approximately 2.5 MHz. This is the size of the largest frequency splitting; most of the splittings are much smaller and lead to unresolved hyperfine patterns producing a linewidth of approximately 1 MHz in the case of naphthalene.[9,24]

### E. General Summary of the Approximations

In Table I we present a general summary of the approximations appropriate to the high-field region,

TABLE I. Proton energy shifts from eigenvalues of $\mathcal{H}_1+\mathcal{H}_2 \equiv \mathbf{G}\cdot\mathbf{S}+\mathbf{S}\cdot\mathbf{T}\cdot\mathbf{S}$ produced by hyperfine interactions of two protons only, in a triplet-state organic molecule, when (a) $\mathbf{H}_0$ is parallel to $\hat{z}$, (b) the molecule is in an electron state which becomes the state $|+\rangle$ at $|\mathbf{H}_0|\to 0$, and (c) both protons have identical tensors $\mathbf{A}_k$ of the form (9).[a]

| | |
|---|---|
| Approximately zero-field region [see (2)] | $\pm\{[-\mathcal{G}_z+(G_z/2E)(A_{1zz}+A_{2zz})]^2+[1/4(D+E)^2](A_{1xx}^2+A_{1xy}^2)(A_{2xx}^2+A_{2xy}^2)\}^{1/2}$ $+(1/8E)(A_{1zz}+A_{2zz})^2+[1/4(D+E)](A_{1xx}^2+A_{1xy}^2+A_{2xx}^2+A_{2xy}^2)$ $\pm\{[(G_z/2E)(A_{1zz}-A_{2zz})]^2+[1/4(D+E)^2](A_{1xx}^2+A_{1xy}^2)(A_{2xx}^2+A_{2xy}^2)\}^{1/2}$ $+(1/8E)(A_{1zz}-A_{2zz})^2+[1/4(D+E)](A_{1xx}^2+A_{1xy}^2+A_{2xx}^2+A_{2xy}^2)$ |
| Low-field region [see (3)] | $\pm\mathcal{G}_z\pm[G_z/2(G_z^2+E^2)^{1/2}](A_{1zz}+A_{2zz})+[1/8(G_z^2+E^2)^{1/2}](A_{1zz}+A_{2zz})^2$ $\pm[G_z/2(G_z^2+E^2)^{1/2}](A_{1zz}-A_{2zz})+[1/8(G_z^2+E^2)^{1/2}](A_{1zz}-A_{2zz})^2$ |
| High-field region [see (4)] | $\pm\mathcal{G}_z\pm[G_z/2(G_z^2+E^2)^{1/2}](A_{1zz}+A_{2zz})$ $\pm[G_z/2(G_z^2+E^2)^{1/2}](A_{1zz}-A_{2zz})$ |

[a] The expressions given above for the electron state which approaches the state $|+\rangle$ as $|\mathbf{H}_0|$ approaches zero may be converted to the expressions applicable to the other states, as follows: For the state which approaches $|-\rangle$ as $|\mathbf{H}_0|$ approaches zero change $A_{kxx}$ to $A_{kyy}$, $2E$ to $-2E$, $D+E$ to $D-E$, in the formulas given above. For the state which approaches $|0\rangle$ as $|\mathbf{H}_0|$ approaches zero change $G_z$ to 0, $A_{kzz}$ to $|A_{kyy}+iA_{kxy}|$, $2E$ to $-(D-E)$, $D+E$ to $-(D+E)$, in the formulas given above. The approximations discussed in the text may be employed to obtain expressions for the cases $\mathbf{H}_0\cdot\hat{\mathbf{x}}=|\mathbf{H}_0|$ and $\mathbf{H}_0\cdot\hat{\mathbf{y}}=|\mathbf{H}_0|$, which are similar to those given in this table for all three electron states for the case $\mathbf{H}_0\cdot\hat{\mathbf{z}}=|\mathbf{H}_0|$.

the low-field region, and the almost-zero-field region, defined by (2), (3), and (4), respectively, as they apply to the particular case of an organic molecule in a triplet state with hyperfine interactions arising from two protons only. The two protons are assumed to have tensors $\mathbf{A}_k$ of the form (9). Table I presents the approximation formulas for the energy shifts from the eigenvalues of $\mathcal{H}_1+\mathcal{H}_2\equiv\mathbf{G}\cdot\mathbf{S}+\mathbf{S}\cdot\mathbf{T}\cdot\mathbf{S}$ in (1) produced by $\mathcal{H}_3+\mathcal{H}_4$ in (1). This collection of formulas displays the manner in which the approximations appropriate to the three different field regions defined by (2), (3), and (4) merge into each other.

## III. THE EXACT TREATMENT FOR ZERO EXTERNAL FIELD

For a particular molecule with known principal values of the tensor $\mathbf{T}$ one may, of course, for an assumed set of tensors $\mathbf{A}_k$, perform an exact calculation of the energy levels and eigenstates of $\mathcal{H}_2+\mathcal{H}_4$ in (1). In the case of a triplet-state molecule such as naphthalene with eight protons, there will be $3\times 2^8=768$ states to consider, and $\mathcal{H}_2+\mathcal{H}_4$ must be diagonalized in this 768-dimensional manifold.

The assumption of planarity and of $D_{2h}$ symmetry for the naphthalene molecule permits a great reduction of the dimensions of the matrices to be diagonalized. We may consider the protons 1, 4, 5, and 8 in Fig. 1. The 16 possible spin states of these four protons generate a 16-dimensional representation of the group $D_{2h}$ under space and spin transformation, which after reduction may be written as

$$+5A_g+2A_u+B_{1g}+2B_{1u}+2B_{2g}+B_{2u}+2B_{3g}+B_{3u}. \quad (22)$$

The protons, 2, 3, 6, and 7 give rise to the same expressions, (22), and the 256-dimensional representation generated by the space and spin transformations on the states of the eight protons thus becomes, after reduction,

$$+44A_g+32A_u+28B_{1g}+32B_{1u}+32B_{2g}+28B_{2u}+32B_{3g}+28B_{3u}. \quad (23)$$

The three electron states, when combined with these 256 proton states, give the 768-dimensional representation, which after reduction may be written as

$$+92A_g+88A_u+108B_{1g}+88B_{1u}+104B_{2g}+92B_{2u}+104B_{3g}+92B_{3u}. \quad (24)$$

A considerable further reduction of the dimensions of the matrices to be diagonalized results from the fact that the proton state operators in the spin Hamiltonian (1) are sums of one-proton operators. Thus, for example, it is possible to divide the states for four protons into the following three sets [(25), (26), (27)] such that the matrix elements of the spin Hamiltonian (1) between any two states of different sets vanish:

nine states belonging to $4A_g+B_{1g}+2B_{2g}+2B_{3g}$, (25)

six states belonging to $2A_u+2B_{1u}+B_{2u}+B_{3u}$, (26)

one state belonging to $A_g$. (27)

TABLE II. Sizes of matrices of spin Hamiltonian, Eq. (1), for naphthalene-$h_8$ with $D_{2h}$ symmetry.

| Number of matrices | Dimensions of matrices |
|---|---|
| 3 | 1 |
| 4 | 5 |
| 4 | 4 |
| 6 | 13 |
| 6 | 14 |
| 4 | 40 |
| 4 | 41 |
| 1 | 56 |
| 2 | 61 |
| 1 | 65 |

Such considerations permit the 768-rowed matrix of the spin Hamiltonian (1) to be reduced to the 35 matrices with the dimensions shown in Table II. The largest matrix to be diagonalized has 65 rows.

## IV. NUMERICAL CALCULATIONS

### A. The Low-Field Range [See Eq. (3)]

It has been pointed out in Sec. II.C that to the approximation which we have used in the low-field region the field splitting in a field scan, constant frequency, EPR experiment, given by (15) for the $k$th proton is independent of the field strength. In the case in which the principal axes of the tensors $\mathbf{A}_k$ are nearly coincident with those of the tensor $\mathbf{T}$ [see (1)], we also expect the EPR hyperfine pattern produced by a set of equivalent protons to be very similar in the high-field [see (2)] and the low-field regions.

As a numerical example we take the proton 1 in Fig. 1 for naphthalene. We use the parameters given in Table III. We consider the case in which $\mathbf{H}_0 \parallel \hat{\mathbf{x}}$.

The spin densities in Table III are taken from Hutchison, Hirota, and Palmer.[24] These spin densities are used with a model in which there are two point spins, one 0.83 Å above and the other 0.83 Å below the planar molecule at each of the C atom positions given in Table III. The dipole–dipole interactions of these spins with protons at the positions given in Table III, plus an isotropic interaction, $-66.9$ MHz[24] per unit spin density on the adjacent C atom, produce the $\mathbf{A}_k$ component values given in Table III. These $\mathbf{A}_k$ component values are not far from those given by Hutchison, Hirota, and Palmer.[24]

Using Eq. (15) in the low-field region and Eq. (8) in the high-field region, we obtain the field splitting values given in Table IV. For protons, $k=1$, 4, 5, and 8 in Fig. 1, the principal axes of $\mathbf{A}_k$ are, for our model, close to (but not exactly) parallel with the principal axes, $\hat{\mathbf{x}}$, $\hat{\mathbf{y}}$, $\hat{\mathbf{z}}$ of $\mathbf{T}$ (see Fig. 1), as is seen from the small value of $A_{1xy}$ in Table III. Thus we see in Table IV the relatively small changes to be expected in the naphthalene proton, $k=1$, 4, 5, 8, hyperfine patterns in EPR spectra in the field range from 5000 to 5 G. In fact the main features of the actually observed hyperfine patterns of naphthalene are determined by these four protons because of the small amount of spin at the other positions, and so we expect the observed field scan EPR hyperfine patterns for naphthalene, when $\mathbf{H}_0 \parallel \hat{\mathbf{x}}$, to be very little changed on going from 5000 to 5 G.

On the other hand, for the protons $k=2$, 3, 6, and 7 in Fig. 1, for which the principal axes of $\mathbf{A}_k$ and $\mathbf{T}$ are not parallel, we find a large variation of the field splitting with $|\mathbf{H}_0|$, $\mathbf{H}_0 \parallel \hat{\mathbf{x}}$.

TABLE III. Naphthalene parameter values used for numerical calculations. Assumed symmetry, $D_{2h}$ (see Fig. 1).

| $k$, position index in Fig. 1 | 1 | 2 | 9 |
|---|---|---|---|
| C $x$ coordinate[29] (Å) | 1.239 | 2.409 | 0.000 |
| C $y$ coordinate[29] (Å) | 1.397 | 0.708 | 0.703 |
| H $x$ coordinate[29] (Å) | 1.240 | 3.352 | ··· |
| H $y$ coordinate[29] (Å) | 2.488 | 1.259 | ··· |
| Spin density[24] | +0.219 | +0.062 | −0.062 |
| $A_{kxx}/h$ (MHz) | −21.37 | −1.01 | ··· |
| $A_{kyy}/h$ (MHz) | −7.23 | −5.78 | ··· |
| $A_{kzz}/h$ (MHz) | −15.36 | −5.65 | ··· |
| $A_{kxy}/h$ (MHz) | −1.62 | +2.33 | ··· |
| $(D+E)/h$ for histogram,[30] Fig. 4 (MHz): 2601.0 | | | |
| $(D+E)/h$ for stick diagram,[31] Fig. 4 (MHz): 2511.9 | | | |
| $(D-E)/h$ for histogram,[30] Fig. 4 (MHz): 3533.0 | | | |
| $(D-E)/h$ for stick diagram,[31] Fig. 4 (MHz): 3439.8 | | | |

TABLE IV. Field splittings produced by naphthalene protons in a constant frequency field scan EPR experiment, $\mathbf{H}_0 \parallel \hat{\mathbf{x}}$ (see Fig. 1), calculated from Table III.

| | Transition | Proton 1 splitting (G) | Proton 2 splitting (G) |
|---|---|---|---|
| Equation (15) 5–350 G | $\sim\|+\rangle\rightarrow\sim\|-\rangle$ or $\sim\|0\rangle\rightarrow\sim\|-\rangle$ | 7.647 | 0.906 |
| Equation (8) 5000 G | $\sim\|0\rangle\rightarrow\sim\|+1\rangle$ | 7.636 | 0.404 |
| | $\sim\|0\rangle\rightarrow\sim\|-1\rangle$ | 7.049 | 0.313 |

### B. The Almost-Zero-Field Range [See Eq. (4)]

It has been pointed out that at zero field, $|\mathbf{H}_0| = 0$, the hyperfine interaction $\mathcal{H}_4$ of only a single proton results in no degeneracy removal, and each of the three electron states remains twofold degenerate. There is, of course, an energy shift produced by the hyperfine interaction. An exact numerical calculation of this shift of the twofold degenerate electron state from its position in the absence of $\mathcal{H}_4$ is presented in the two left-hand columns of Fig. 2 for two cases with $|\mathbf{H}_0| = 0$. In the first case the single proton is assumed to have the $\mathbf{A}_1$ of proton 1 in Fig. 1 with numerical values of components given in Table III. In the second case the parameter values for proton 2 are assumed to hold for the single proton.

When only two protons are considered there is complete degeneracy removal by $\mathcal{H}_4$. An exact numerical calculation of the resulting shifts from the energies of the fourfold degenerate electron states in the absence of $\mathcal{H}_4$ is presented in the two right-hand columns of Fig. 2 for two cases with $|\mathbf{H}_0| = 0$. In the first case, one of the only two protons is assumed to have the $\mathbf{A}_1$ of proton 1 in Fig. 1 with the numerical values of components given in Table III. The other of the only two protons is assumed to have the $\mathbf{A}_2$ of proton 2. In the second case, both of the protons are assumed to have the $\mathbf{A}_k$ of proton 1.

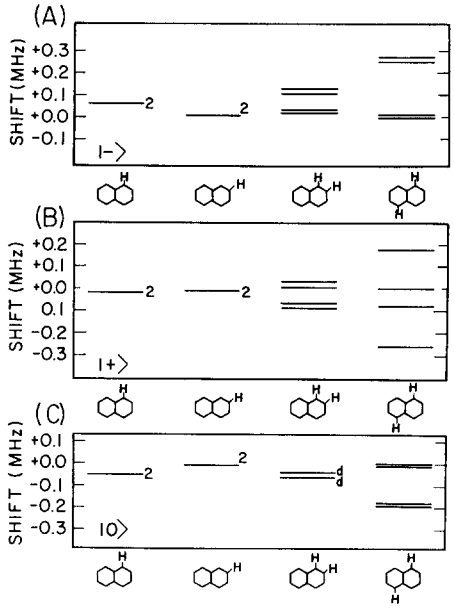


FIG. 2. Proton hyperfine shifts and splittings produced by one proton only (two left-hand columns) and by two protons only (two right-hand columns) in the naphthalene-$h_8$ triplet-state molecule at zero external magnetic field. (A) Shifts and splittings for state $|-\rangle$; (B) shifts and splittings for state $|+\rangle$; (C) shifts and splittings for state $|0\rangle$.

The two important features, (I) and (II), of zero-field EPR spectra mentioned previously at the end of Sec. II.D, are apparent in this numerical calculation.

For the last two-proton case mentioned above which is presented in the last column on the right of Fig. 2 we have also considered numerically the effect of a small magnetic field in the almost-zero-field range. These results are presented in Fig. 3 for $\mathbf{H}_0$ parallel to the $\hat{\mathbf{z}}$ axis. The variations of energy with field are such that the changes between 0 and 2 G are about the size of the level separations at zero field. Thus fields as small as 2 G will produce drastic changes in ENDOR spectra from those obtained at exactly zero field. In a randomly oriented collection of triplet-state molecules the anisotropy broadening of the ENDOR lines by a 2G field could be as large as the line frequency.

We have made exact calculations of the frequencies and intensities of the EPR absorption lines, at exactly zero external magnetic field, produced by a naphthalene triplet-state molecule with only the four protons 1, 4, 5, 8 of Fig. 1. We have used the parameter values given in Table III for proton 1, assuming $D_{2h}$ symmetry to generate the $\mathbf{A}_k$ for protons 4, 5, and 8. Three such calculations were made with the "stick diagram" $D+E$ and $D-E$ values given in Table III and for microwave magnetic field polarization directions parallel to $\hat{\mathbf{x}}$, $\hat{\mathbf{y}}$, and $\hat{\mathbf{z}}$ of Fig. 1. There is a very large number of transitions but for each of the three polarizations there are 16 intense transitions of almost equal intensity, each of which is at least 100 times as intense as the less intense transitions. The total intensity of these less intense transitions is not great enough to make an appreciable contribution to the line shape. The frequencies of these 16 transitions for each microwave magnetic field polarization have been indicated in Fig. 4 by the positions of vertical sticks of unit height. Three degeneracies and some near degeneracies occur for each polarization and are represented by sticks of two and three times the unit height.

We have calculated the eigenvalues and eigenstates of the 768-by-768 matrix of $\mathcal{H}_2+\mathcal{H}_4$ [see (1)] for triplet-state naphthalene, which was discussed in detail in Sec. III. Table II gives the sizes of the matrices which were diagonalized. The values of $\mathbf{A}_1$ and $\mathbf{A}_2$ components and the "histogram values" of $D+E$ and $D-E$, which are listed in Table III, were used. Inasmuch as the energy shifts from the eigenvalues of $\mathcal{H}_2$ only are very small, double precision computer programs were employed to obtain sufficiently accurate eigenvalues and eigenstates. The intensities of all transitions associated with frequencies in the vicinity of $(D+E)/h$, $(D-E)/h$, and $2E/h$ were calculated for microwave magnetic field polarizations parallel to $\hat{\mathbf{x}}$, $\hat{\mathbf{y}}$, and $\hat{\mathbf{z}}$ of Fig. 1.

The results of this calculation are presented in histogram form in Fig. 4.

It has been mentioned in Sec. II.A above that if $\mathbf{g}_a$ which occurs in $\mathbf{G}$ in the spin Hamiltonian (1) is not isotropic, then in general $\mathbf{A}_k$ in (1) will not be symmetric. We have assumed in (9) above, and elsewhere, that $\mathbf{A}_k$ is symmetric. Off-diagonal elements of the $\mathbf{A}_k$ such as $A_{xy}$ and $A_{yx}$ enter these calculations through

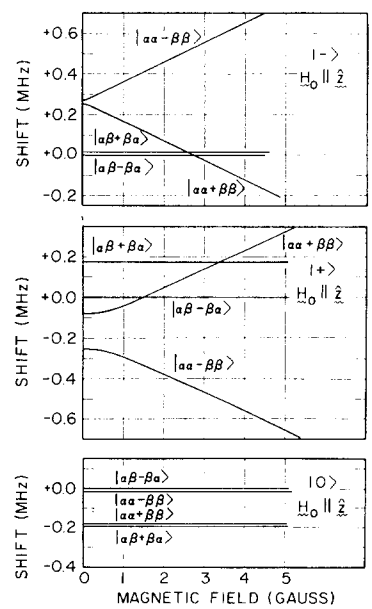


FIG. 3. The effect of a small external magnetic field, parallel to the $z$ axis, on proton hyperfine splittings produced by two protons only, in the naphthalene-$h_8$ triplet-state molecule. The top, middle, and bottom portions of this figure show the effect of $\mathcal{H}_3+\mathcal{H}_4$ on the eigenvalues of $\mathcal{H}_1+\mathcal{H}_2$ in the cases of the electron states $\sim|-\rangle$, $\sim|+\rangle$, and $\sim|0\rangle$, respectively.

relations such as those expressed in (15) above, in the combinations $A_{xx}+iA_{xy}$ or $A_{yy}+iA_{yx}$ with diagonal elements. The contributions to the energy are proportional to $|A_{xx}+iA_{xy}|^2$ or $|A_{yy}+iA_{xy}|^2$. Thus the calculations of energies and frequencies which assume that $\mathbf{g}_e$ is isotropic with value $g_e=2.00238$, and therefore that $\mathbf{A}_k$ is symmetric, must be corrected by the factor $|g_{xx}/g_e|^2$ or $|g_{yy}/g_e|^2$ or $|g_{zz}/g_e|^2$ to give the values obtained for the not-symmetric $\mathbf{A}_k$ appropriate to an anisotropic $\mathbf{g}_e$ with principal values $g_{xx}$, $g_{yy}$, and $g_{zz}$. We may make an estimate of the approximate values of such correction factors for the largest reported anisotropies of $\mathbf{g}_e$ for a photoexcited aromatic molecule, namely, for phenanthrene in diphenyl,[6,9] in which case these factors are 1.0004, 1.0017, and 0.9997, respectively. Thus a typical calculated energy level or frequency shift of $\sim$1 MHz if calculated assuming an isotropic $g_e$ value 2.0024 would in this case be in error by at most 2 kHz. The reported anisotropies in $\mathbf{g}_e$ for photoexcited naphthalene[9] are much smaller than the anisotropies assumed in this estimate.

## V. EPR EXPERIMENTS

### A. Experiments at Zero External Magnetic Field

Single crystals of naphthalene in diphenyl-$h_{10}$, durene-$d_{14}$, and naphthalene-$d_8$ were prepared by the methods described by Brandon, Gerkin, and Hutchison[6] from zone-refined materials. The melts from which the crystals were grown contained 1.0 mol% naphthalene.

The zero-field spectrometer, developed in this laboratory and used in these experiments, has been previously described.[7] The earth's magnetic field at the sample was canceled to within 10 mG. The bidirectional square wave modulation field (see Ref. 7) contributed $<35$ mG to the field at the sample during the measurement (field off) portion of the modulation cycle. Frequency errors were not greater than $2.5\times10^{-7}$ times the frequency.

The $Q$ of the cavity[7] was normally in the range from $\sim$800 to $\sim$1200. The microwave magnetic field amplitude at the sample was varied between estimated values of 150 and 2 mG for the several measurements. The polarization of the microwave magnetic field at the sample was approximately along the appropriate fine structure principal axis for the transition being studied,[6] for one of the two molecules per unit cell.

For the transitions at frequencies $(D+E)/h$ and $(D-E)/h$, the frequency was swept at rates 9.4 and 11.6 kHz sec$^{-1}$, respectively, and a time constant 2.5 sec was used for the detection. For the transition at frequency $2E/h$, the sweep rate was 3.4 kHz sec$^{-1}$ and the time constant was 22 sec.

It is necessary that the frequency of maximum EPR absorption during the "field-on" portion of the bidirectional square wave cycle[7] be sufficiently different from the frequency for zero-field EPR absorption during the "field-off" portion to permit the obtaining of undistorted zero-field line shapes. This was assured in the present measurements by optimal orientation of the direction of the modulation field with respect to the fine-structure tensor principal axes[6] and by locating the modulation coil[7] closer to the sample than was the case for the previously reported measurements,[7,9] thus providing a larger square wave field. The previously reported frequency widths[7,9] of zero-field lines are seriously inaccurate due to overlapping of the "on-field" line with the observed zero-field line, which made some lines appear to be considerably narrower than their true width.

The naphthalene molecules were photoexcited to the triplet state by a 500-W Osram HBO 500 mercury arc. The light was filtered by a 5-cm path length of a solution which contained 90 g liter$^{-1}$ of $NiSO_4\cdot6H_2O$ and 18 g liter$^{-1}$ of $CoSO_4\cdot7H_2O$ in $H_2O$ to reduce heating of the sample.[32]

Measurements were made at two temperatures, 1.584°K [33] (with an estimated standard deviation, 0.002°K) and near the boiling point of $N_2$. For the 1.584°K [33] measurements the sample crystal was in direct contact with the He liquid. For the measurements at the higher temperature it was necessary to exclude $N_2$ liquid from the microwave cavity. The temperature was measured with a thermocouple under the same conditions as for the EPR measurements and found to be 83.1°K (with an estimated standard deviation of 0.5°K). The sizes of thermal gradients over the samples under these last conditions were unknown. Such gradients would produce line broadenings which would be considerably less for the transitions at frequency $(D+E)/h$ than for those at $(D-E)/h$ because for naphthalene-$d_8$ in diphenyl at this temperature the value of $\partial(D-E)h^{-1}/\partial T$ is $-0.30$ MHz deg$^{-1}$ [28] and the value of $\partial(D+E)h^{-1}/\partial T$ is $-0.083$ MHz deg$^{-1}$.[28]

In Table V we have summarized the observations on linewidths at zero external magnetic field for the transition at frequency $(D+E)/h$ in the case of naphthalene.

In Fig. 4 we have presented the experimental chart recordings for all three EPR transitions for triplet-state naphthalene-$h_8$ in zero external magnetic field at $\sim$83°K. The conditions of measurement for the frequencies $(D+E)/h$ and $(D-E)/h$ as given in Fig. 4 are those given in Row 5 of Table V. The measurement for frequency $2E/h$ was made in a larger (by factor 2 in linear dimensions) cavity than that referred to above.

### B. Experiments in the Low-Field and Almost-Zero-Field Ranges

The experiments in the low-field and almost-zero-field ranges [see (3) and (4) above] which are pertinent to the previous discussions of this paper have been reported by Gerkin and Winer.[16] They have described the hyperfine structure of that EPR line of triplet-state

TABLE V. Summary of experimental observations of typical linewidths of the EPR absorption in single crystals for the triplet-state naphthalene molecule at frequency $(D+E)/h$ in zero external magnetic field.

| Row number | Naphthalene guest | Host | $T$ (°K) | Signal-to-noise ratio | Microwave field at sample (mG) | Width at 1/2 height[a] (MHz) |
|---|---|---|---|---|---|---|
| 1 | $-h_8$ | Naphthalene-$d_8$ | 1.584 | ~30 | ~2 | 1.25 |
| 2 | $-h_8$ | | 1.584 | ~50 | ~15 | 1.45 |
| 3 | $-h_8$ | Diphenyl-$h_{10}$ | 1.584 | ~20 | ~150 | 2.85 |
| 4 | $-h_8$ | | 1.584 | ~5 | ~5 | 1.6 |
| 5 | $-h_8$ | | 83.1 | ~225 | ~100 | 1.28 |
| 6 | $-h_8$ | Durene-$d_{14}$ | 1.584 | ~200 | ~150 | 2.16 |
| 7 | $-h_8$ | | 1.584 | ~250 | ~50 | 1.72 |
| 8 | $-h_8$ | | 1.584 | ~170 | ~15 | 1.64 |
| 9 | $-h_8$ | | 1.584 | ~70 | ~5 | 1.46 |
| 10 | $-d_8$ | Diphenyl-$h_{10}$ | 83.1 | ~400 | ~150 | 0.66 |
| 11 | $-d_8$ | Durene-$d_{14}$ | 1.584 | ~80 | ~150 | 0.90 |
| 12 | $-d_8$ | | 1.584 | ~700 | ~8 | 0.83 |
| 13 | $-d_8$ | | 83.1 | ~100 | ~150 | 4.3 |
| 14 | $-d_8$ | Polymethylmethacrylate glass | 1.584 | ~10 | ~150 | ~25. |

[a] For signal-to-noise ratios 50 or larger, the estimated standard deviation of this value is 0.07 MHz. For smaller signal-to-noise ratios the deviation is larger.

naphthalene-$h_8$ whose frequency approaches the value $(D-E)/h$ as the external magnetic field is reduced to zero. They have used a field scanning technique to present chart recordings of this line with the external field parallel to the $\hat{\mathbf{x}}$ axis of naphthalene (see Fig. 1), and give hyperfine patterns, presumably obtained for five different fixed frequencies corresponding to five different field scan ranges below 100 G. They comment on the similarity between the proton hyperfine patterns which they obtained at these low fields and the results which they obtained in the high-field region [see (2) above].

## VI. DISCUSSION

### A. Line Shapes in Zero External Magnetic Field

It is clear from the numerical calculations in Sec. IV above, which have been presented in Fig. 4, that in order to observe any proton hyperfine structure in the EPR spectrum of triplet-state naphthalene-$h_8$ at zero external magnetic field it is necessary that the line broadening mechanisms which are present give linewidths less than about 1–2 MHz. We see from Table V that experimental linewidths in single crystals are of approximately this size. It is apparent that a number of line broadening mechanisms may be producing effects in these measurements. Inhomogeneous crystal strains, magnetic fields of nuclei of host molecules, temperature gradients created by illumination, and microwave power saturation are a few of the sources of broadening which may be mentioned. However, it is clear from the data in Row 10 of Table V for naphthalene-$d_8$ in a diphenyl-$h_{10}$ host crystal, in which a linewidth 0.66 MHz is observed, that it is possible to obtain sufficiently small residual linewidths to permit observation of proton hyperfine interaction effects on the line shape for naphthalene-$h_8$ in diphenyl-$h_{10}$.

Figure 4 shows the observed proton hyperfine structure effects on line shapes observed for naphthalene-$h_8$ in diphenyl-$h_{10}$ at 83°K. The experimental conditions are those given in Row 5 of Table V. In Fig. 4 comparison is made with the exact zero-field calculation described in Sec. IV. B as well as with the four-proton calculation which is also described in Sec. IV.B.

The striking agreement of these observations with the calculations is apparent. Among the marked features of the calculations which are verified by the experiments are: (a) the bump on the high-frequency side of the transition at $(D+E)/h$, (b) the sharp cutoff on the low-frequency side of the transition at $(D-E)/h$, and (c) the long high-frequency tail on the transition at $2E/h$. Thus the calculations which are based on the experimentally well-known properties of the naphthalene triplet-state molecule in the high-field range [see (2) above] lead to predictions concerning observed line shapes at zero external magnetic field which are verified by these measurements.

The histograms which are shown in Fig. 4 and which summarize the exact numerical calculations of Sec.

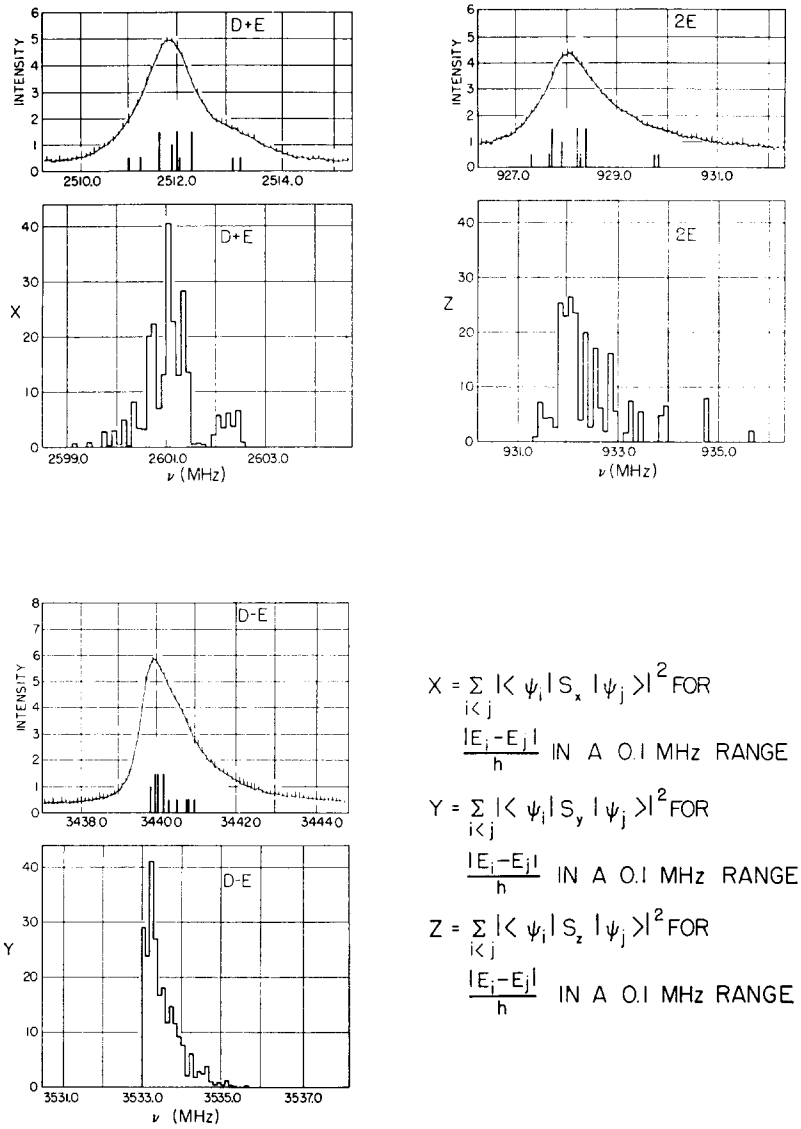


FIG. 4. (a) Experimental chart recordings of EPR absorption lines for the naphthalene-$h_8$ triplet-state molecules in a single diphenyl-$h_{10}$ crystal in zero external magnetic field at ~83°K. These are the three smooth curves with frequency markers at 100-kHz intervals for the three EPR transitions at frequencies $(D+E)/h$, $(D-E)/h$, and $2E/h$. Experimental conditions are given in Row 5 of Table V. (b) Calculated absorption frequencies and intensities at exactly zero external magnetic field for naphthalene triplet-state molecules in a single diphenyl-$h_{10}$ crystal at 83.1°K [31] produced by only the four protons 1, 4, 5, 8 (see Fig. 1). These are the vertical stick diagrams. (c) Calculated absorption frequencies and intensities at exactly zero external magnetic field for naphthalene-$h_8$ triplet-state molecules, including all protons, using the histogram $D$ and $E$ values[30] from Table III. These are the histograms. The histograms labeled $D+E$, $D-E$, and $2E$ give the total intensity in each 0.1-MHz frequency range for microwave magnetic field polarization along $\hat{x}$, $\hat{y}$, and $\hat{z}$, respectively.

IV.B above were prepared using $D$ and $E$ values[30] close to those experimentally observed at 1.584°K[33] for naphthalene-$d_8$ in durene-$d_{14}$. [See Table III above.] This accounts for the discrepancy in frequency scale position for the histogram and the experimental recording for the different system. However, the A components which were chosen were typical for naphthalene. There would be no appreciable line shape changes for a choice of $D$ and $E$ values in agreement with the experimental values[31] for naphthalene-$h_8$ in diphenyl-$h_{10}$ because of the very small difference between these latter values and those used (see Table III and Refs. 30 and 31), and because of the relatively very small dependence of the line shape on $D$ and $E$ values.

When considering the experimental results which are summarized in Table V the following points are to be noted.

The measurements made at temperatures below the λ point of He indicate that the observed transitions are possibly being saturated, leading to width values which are not the true values of the unsaturated lines. This saturation has prevented the observation of hyperfine structure effects on line shapes below the λ point. The regenerative microwave spectrometer[7] which was used for these measurements (see Sec. V.A above) will not oscillate below a power level which is sufficient to give saturation at these lowest temperatures.

In view of the fact that the linewidths and shapes of lines observed at ~83°K for naphthalene-$h_8$ in diphenyl-$h_{10}$ are accounted for by the proton hyperfine interactions, it is to be assumed that the observed widths and shapes of lines observed at the same temperature for naphthalene-$d_8$ in diphenyl-$h_{10}$ are probably due, in the main, to the deuteron hyperfine interactions (dipole and quadrupole). The narrower lines which are observed in this case are to be expected on this assumption.

The linewidths reported in Rows 3, 4, 13, and 14 of Table V are anomalously large. In the case of naphthalene-$h_8$ in diphenyl-$h_{10}$ at 1.58°K[33] reported in Rows 3 and 4 it is presumed that these large widths have their origins in multiple (but discrete) orientations of guest molecules at host molecule sites.[34,35] In the case of naphthalene-$d_8$ in durene-$d_{14}$ at ~83°K reported in Row 13 the great linewidth may be due to modulation of the local field or crystal field[36] by rotations of methyl groups[37] on the host durene molecules. It is probable that a structural change occurs in durene at a temperature somewhere between 1.58 and ~83°K as evidenced by both the drastic difference between the linewidths listed in Row 13 and in Rows 11 and 12 and by the existence of a very large discontinuity in the temperature dependences of $D$ and $E$ for naphthalene between ~83 and 1.58°K[23] for the durene-$d_{14}$ host.

In the case of the linewidth reported in Row 14 for naphthalene in polymethylmethacrylate glass the large value is presumably caused by an inhomogeneous broadening arising from strains in the host.

### B. Proton Hyperfine Structure in the Low-Field Range

The considerations of Secs. II.C and IV.A above have led to the conclusion that for triplet-state naphthalene-$h_8$ we expect little change, in the range from 5000 down to 5 G, in the general appearance of the proton hyperfine patterns obtained in fixed-frequency field scan experiments when $\mathbf{H}_0 \| \hat{\mathbf{x}}$ (see Fig. 1). The measurements of Gerkin and Winer[16] for naphthalene-$h_8$, which have been described in Sec. V.B, show excellent agreement with these expectations. The naphthalene protons $k=1$, 4, 5, 8 (see Fig. 1) whose principal axes of the $\mathbf{A}_k$ are very close to being parallel to the principal axes of $\mathbf{T}$ give almost unchanged splittings in this range. This result is presented in Table IV. These are the protons at the positions of high spin density and so the general appearance (e.g., five peaks) of the patterns is unaltered as the field is reduced. On the other hand, the protons $k=2$, 3, 6, 7 at the positions of low spin density have principal axes of the $\mathbf{A}_k$ which are very far from being parallel to the principal axes of $\mathbf{T}$, and they show greatly increased splittings at the lower fields, $>5$ G, as presented in Table IV. This of course accounts for the loss of resolution observed by Gerkin and Winer[16] at fields of 10 or 20 G. The loss of structure at fields of ~5 G is also clearly understood through the considerations of Secs. II.D, III, and IV.B. Gerkin and Winer's[16] lowest field scan goes down from an initial field of order 20 G and so, of course, shows some resolved structure at the beginning of the scan, and as expected, the absorption covers a field range which is, as they say, "comparable to the range spanned by the corresponding portion" of the patterns obtained at higher fields. However, any impression, obtained from such a statement,[16] that there is an immutable "hyperfine pattern" of fixed width and fixed general appearance, with a "(central) field" which moves to lower and lower values as the fixed scan frequency is lowered, permitting one to see a "portion" only of this pattern when the "(central) field" is less than half the width (~35 G) of the somewhat higher field pattern, is of course completely erroneous. This is very clear from our discussions in Sec. II.D above.

## ACKNOWLEDGMENTS

We thank Dr. Valda H. McCann for growing some of the crystals used in the experiments, Dr. Charles G. Wade for assistance in some of the measurements, Clark E. Davoust for construction of electronic equipment, Warren Geiger for construction of apparatus, and the Computation Center of the University of Chicago for the programming of calculations. Acknowledgment is made to the donors of The Petroleum Research Fund, administered by the American Chemical Society, for partial support of this research.

* This research has been supported by the U.S. Atomic Energy Commission.

† Electronic equipment used in the experimental work has been supplied by the Advanced Research Projects Agency.

‡ Present address: Physics Department, Queen's University, Belfast, BT7 1NN, Northern Ireland.

§ National Science Foundation Predoctoral Fellow, 1965–1969.

[1] R. W. Brandon, R. E. Gerkin, and C. A. Hutchison Jr., J. Chem. Phys. **37,** 447 (1962).

[2] P. Csavinsky, *Luminescence of Organic and Inorganic Materials*, edited by H. P. Kallman and G. M. Spruch (Wiley, New York, 1962), p. 263.

[3] C. A. Hutchison Jr., *Proceedings of the Xth Colloquium Spectroscopium Internationale* (Spartan Books, 1963), p. 681.

[4] C. A. Hutchison Jr., Rec. Chem. Progr. **24,** 105 (1963).

[5] D. D. Thomas, A. W. Merkl, A. F. Hildebrandt, and H. M. McConnell, J. Chem. Phys. **40,** 2588 (1964).

[6] R. W. Brandon, R. E. Gerkin, and C. A. Hutchison Jr., J. Chem. Phys. **41,** 3717 (1964).

[7] L. E. Erickson, Phys. Rev. **143,** 295 (1966).

[8] J. H. van der Waals and M. S. de Groot, *The Triplet State*, edited by A. B. Zahlan (Cambridge U. P., Cambridge, England, 1967), pp. 101, 172.

[9] C. A. Hutchison Jr., *The Triplet State*, edited by A. B. Zahlan (Cambridge U. P., Cambridge, England, 1967), p. 63.

[10] R. E. Gerkin and A. M. Winer, J. Chem. Phys. **47,** 2504 (1967).

[11] J. Schmidt and J. H. van der Waals, Chem. Phys. Letters **2,** 640 (1968).

[12] J. Schmidt and J. H. van der Waals, Chem. Phys. Letters **3,** 546 (1969).

[13] D. S. Tinti, M. A. El-Sayed, A. H. Maki, and C. B. Harris, Chem. Phys. Letters **3,** 343 (1969).

[14] R. E. Gerkin and P. Szerenyi, J. Chem. Phys. **50,** 4095 (1969).

[15] R. E. Gerkin and A. M. Winer, J. Chem. Phys. **50,** 3114 (1969).

[16] R. E. Gerkin and A. M. Winer, J. Chem. Phys. **51,** 1664 (1969).

[17] I. Y. Chan, J. Schmidt, and J. H. van der Waals, Chem. Phys. Letters **4,** 269 (1969).

[18] C. B. Harris, D. S. Tinti, M. A. El-Sayed, and A. H. Maki, Chem, Phys. Letters **4,** 409 (1969).

[19] L.-T. Cheng and A. L. Kwiram, Chem. Phys. Letters **4,** 457 (1969).

[20] T. S. Kuan, D. S. Tinti, and M. A. El-Sayed, Chem. Phys. Letters **4,** 507 (1970).

[21] J. Schmidt, W. S. Veeman, and J. H. van der Waals, Chem. Phys. Letters **4,** 341 (1969).

[22] M. J. Buckley, C. B. Harris, and A. H. Maki, Chem. Phys. Letters **4,** 591 (1970).

[23] C. A. Hutchison Jr. and B. W. Mangum, J. Chem. Phys. **29,** 952 (1958); **34,** 908 (1961).

[24] N. Hirota, C. A. Hutchison Jr., and P. Palmer, J. Chem. Phys. **40,** 3717 (1964).

[25] C. A. Hutchison Jr. and G. A. Pearson, J. Chem. Phys. **47,** 520 (1967).
[26] A. M. Ponte Goncalves and C. A. Hutchison Jr., J. Chem. Phys. **49,** 4235 (1968).
[27] C. A. Hutchison Jr. and B. E. Kohler, J. Chem. Phys. **51,** 3327 (1969).
[28] C. A. Hutchison Jr., G. W. Scott, and C. G. Wade (personal communication).
[29] D. W. J. Cruickshank, Acta Cryst. **10,** 504 (1957).
[30] C. A. Hutchison Jr. and G. W. Scott (personal communication); in zero external magnetic field at 1.584°K [33] for naphthalene-$d_8$ in durene-$d_{14}$, the maxima of the absorptions at frequencies near $(D+E)/h$ and $(D-E)/h$ have values 2599.54 and 3532.3 MHz, respectively, with standard deviations 0.05 and 0.3 MHz, respectively.
[31] These values of $(D+E)/h$ and of $(D-E)/h$ were chosen to give a close fit to the experimentally observed spectra (see Sec. VI.A and Fig. 4).
[32] M. Kasha, J. Opt. Soc. Am. **38,** 929 (1948).
[33] The temperature was determined by interpolation of vapor pressure data for helium given in G. K. White, *Experimental Techniques in Low Temperature Physics* (Oxford U. P., Oxford, England, 1959), p. 105. The measured vapor pressure of He in these experiments was 5.30 mm Hg.
[34] R. M. Hochstrasser and G. J. Small, J. Chem. Phys. **48,** 3612 (1968).
[35] C. A. Hutchison Jr., V. H. McCann, and G. W. Scott (personal communication).
[36] R. J. Clarke, R. M. Hochstrasser, and C. J. Marzzacco, J. Chem. Phys. **51,** 5015 (1969).
[37] P. S. Allen and A. Cowking, J. Chem. Phys. **49,** 789 (1968).

THE JOURNAL OF CHEMICAL PHYSICS VOLUME 53, NUMBER 5 1 SEPTEMBER 1970

# Neutron-Diffraction Study of $D_3Co(CN)_6$

H. U. GÜDEL AND A. LUDI
*Institut für Anorganische, Analytische, und Physikalische Chemie der Universität, Freiestrasse 3, CH-3000 Bern, Switzerland*
AND
P. FISCHER AND W. HÄLG
*Delegation AF, Eidgenössisches Institut für Reaktorforschung, CH-5303 Würenlingen, Switzerland*
(Received 27 January 1970)

The crystal structure of $D_3Co(CN)_6$ has been determined by a neutron-diffraction analysis of a polycrystalline sample at room temperature. The deuterated compound was prepared from $H_3Co(CN)_6$. It crystallizes according to space group $D_{3d}^1$-$P\bar{3}1m$ with $a=6.431(4)$ Å and $c=5.695(4)$ Å. The lattice constants do not show any isotope effect within the limits of error. Slightly trigonally distorted $Co(CN)_6$ octahedra are three-dimensionally linked by N–D–N bonds. The Co–C, C–N, and N–N distances are 1.88, 1.15, and 2.60 Å, respectively. The latter distance is the shortest so far found in an N–D–N or N–H–N bond. These hydrogen bonds are either linear symmetric or statistically asymmetric (double minimum) centered on $(\frac{1}{2}, 0, \frac{1}{2})$.

## I. INTRODUCTION

The study of the N–H–N hydrogen bond by infrared spectroscopy in a variety of hydrogen hexacyanometalates has been the subject of several investigations.[1–3] For the specific case of $H_3Co(CN)_6$ and corresponding acids of other tervalent metal ions, the spectrum shows a sharp single band due to the stretching vibration of the cyanide ion and a broad absorption between about 1900 and 600 $cm^{-1}$. This broad absorption, which does not exhibit a pronounced structure and which does not change significantly upon deuteration, has been interpreted as evidence for a short and strong N–H–N hydrogen bond. By comparison with compounds containing O–H–O bridges it was concluded that this broad absorption might be caused by a symmetric N–H–N bond.[1,2] Other authors also discussed a high mobility of the protons in the crystal in connection with the infrared spectrum.[3]

The existence of Co–C–N–H bridges shows up in the infrared spectrum.[4] The stretching vibration $\nu$(CN) is shifted about 70 $cm^{-1}$ towards higher wavenumbers compared with the infrared spectrum of the mononuclear $K_3Co(CN)_6$. On the other hand, almost identical spectra are observed for the two compounds in the ultraviolet region,[5] indicating that the coordination polyhedra of both compounds are $Co(CN)_6$ octahedra.

The x-ray powder pattern of $H_3Co(CN)_6$ has been indexed on the basis of a primitive hexagonal unit cell containing one formula unit, with the lattice constants $a=6.431\pm0.004$ Å and $c=5.695\pm0.004$ Å.[6] Using these data and stereochemical arguments, Pauling and Pauling postulated a structural model showing a relationship to the cubic unit cell of prussian blue.[7] The determination of the crystal structure of $H_3Co(CN)_6$ by x-ray powder techniques confirmed this postulated structure.[5] The hydrogen atoms, however, could not be located. The resulting structure can be described as belonging to space group $D_{3d}^1$-$P\bar{3}1m$,[8] with Co at the special position 1*a* (0, 0, 0), C and N at 6*k* $(x, 0, z)$. Cobalt is coordinated approximately octahedrally by six cyanide ions. These coordination polyhedra are expected to be linked together by N–H–N hydrogen bonds leading to a three-dimensional network. The most probable bonds correspond to the shortest N–N distances in the lattice of $H_3Co(CN)_6$. The correspond-